

Published in final edited form as:

Anal Chem. 2009 October 1; 81(19): 8236–8243. doi:10.1021/ac901634y.

Simultaneous Separation of Negatively and Positively Charged Species in Dynamic Field Gradient Focusing Using a Dual Polarity Electric Field

Jeffrey M. Burke¹, Zheng Huang², and Cornelius F. Ivory^{1,*}

¹Gene and Linda Voiland School of Chemical Engineering and Bioengineering, Washington State University, Pullman, WA, USA

²Genzyme Corporation, Framingham, MA, USA

Abstract

Dynamic field gradient focusing (DFGF) utilizes an electric field gradient established by a computer-controlled electrode array to separate and concentrate charged analytes at unique axial positions. Traditionally, DFGF has been restricted to the analysis of negatively charged species due to limitations in the software of our voltage controller. This paper introduces a new voltage controller capable of operating under normal polarity (positive potentials applied to the electrode array) and reversed polarity (negative potentials applied to the electrode array) for the separation of negatively and positively charged analytes, respectively. The experiments conducted under normal polarity and reversed polarity illustrate the utility of the new controller to perform reproducible DFGF separations (elution times showing less than 1% run-to-run variation) over a wide pH range (3.08 to 8.5) regardless of the protein charge. A dual polarity experiment is then shown in which the separation channel has been divided into normal polarity and reversed polarity regions. This simultaneous separation of negatively charged R-phycoerythrin (R-PE) and positively charged cytochrome c (CYTC) within the same DFGF apparatus is shown.

Introduction

Dynamic field gradient focusing (DFGF)¹ is an electric field gradient focusing (EFGF)² technique in which an electric field gradient and an opposing hydrodynamic flow focus charged analytes to unique axial positions. Unlike other EFGF techniques which use shaped channels²⁻⁵, conductivity gradients^{6,7} or temperature gradients⁸⁻¹³ to generate the electric field gradient, DFGF uses a computer-controlled electrode array which allows manipulation of the electric field profile during the course of an experiment to increase resolution or to elute individual species.

The first DFGF apparatus was described by Huang and Ivory¹. This device used 50 controllable electrodes and an 8 cm separation channel to focus a cocktail of proteins. Myers and Bartle¹⁴ expanded this idea by introducing a miniaturized DFGF apparatus containing only 5 electrodes in which they demonstrated the successful separation of Kaleidoscope[®] prestained proteins. An even simpler apparatus consisting of a separation channel with two intersecting side-channels was introduced by Petsev et al¹⁵. By carefully controlling the voltage at each intersection, they were able to successfully separate R-phycoerythrin (R-PE) and fluorescein isothiocyanate conjugated bovine serum albumin (FITC-BSA).

*Corresponding author. Phone: (509) 335-7716. cfivory@wsu.edu.

Tracy and Ivory^{16–19} developed a preparative scale DFGF apparatus capable of separating tens to hundreds of milligrams of protein. Unlike other DFGF devices which have traditionally used chromatographic media to reduce band broadening, this device utilized a turning rotor within a stationary cylinder to produce vortices which introduced controlled radial dispersion to reduce axial dispersion. Using this strategy, they demonstrated the successful separation of 7 mg each of hemoglobin and FITC-BSA.

Burke and Ivory²⁰ have recently developed a 2D nonlinear numerical simulation of DFGF which was used to examine some of the bottlenecks that gave way to decreased system performance and reproducibility problems. Using this simulation, they examined the difference between the potential applied at the electrodes and the potential measured in the separation channel, termed voltage degradation. Two contributions to voltage degradation, electrode spacing and the defocusing region, which is where the field reverses slope and serves to disperse rather than focus peaks, were studied. They found that the shape of the field could be optimized with minimal voltage degradation and that the defocusing zone could be minimized by carefully choosing the distance of the electrodes from the separation channel and by the addition of a negative potential electrode following the ground electrode.

In addition, they compared the results of peaks eluted past a detector using voltage controlled elution (shallowing of the electric field gradient) and peaks eluted under constant electric field gradient. They found that voltage controlled elution gave rise to overly resolved peaks with decreased concentration, an artifact of shallowing the electric field gradient. Peaks eluted under a constant electric field gradient maintained their shape and resolution through the elution process, resulting in more concentrated peaks.

In a separate publication, Burke and Ivory²¹ used the 2D numerical simulation to examine the impact of the dialysis membrane on DFGF performance. Specifically, they looked at membrane stability, polarization of protein onto the surface of the membrane, and the effect of membrane resistance on the shape of the electric field measured in the separation channel. They found that the structural characteristics and the charge on the membrane had a large impact on run-to-run reproducibility and on the shape of the electric field.

Through this work and the work of other groups on the optimization of experimental parameters²², a reproducible and robust DFGF system has been developed. However, these devices as well as almost all EFGF devices have been operated at alkaline pH to ensure that the species being analyzed are negatively charged. When performing under these conditions, positive potentials are applied to the electrodes, which behave as anodes and this will be referred to as normal polarity in this paper. Operation under normal polarity works for many samples; however, the analysis of basic proteins can be difficult due to the high pHs that would have to be used to ensure that the species remain negatively charged.

Alternately, a low pH buffer could be used so that the analytes, now positively charged, could be separated in a reversed polarity field where negative potentials have been applied to the electrodes. This setup is relatively straightforward in EFGF devices which utilize only one power supply, such as those that use shaped channels or conductivity gradients, as long as the voltage source is capable of dual-polarity. A reverse polarity separation of positively charged proteins in a shaped channel EFGF apparatus was illustrated by Lin et al²³ for the separation of lysozyme and myoglobin in 20 mM acetate buffer at pH 4.3 with an applied voltage of -2 kV. Through optimization of the voltage controlled elution protocol, they were able to achieve baseline resolution of these two proteins.

With DFGF, analysis of positively charged species has not been possible because of limitations in the software of the original voltage controller²⁴. This paper introduces a new voltage controller designed for the application of negative or positive potentials. A series of

protein separations will be used to illustrate the ability of DFGF to separate negatively or positively charged species using this new controller.

In addition, dual polarity operation will be demonstrated by simultaneous separation of both negatively and positively charged species within the same separation device. This is achieved by specifying a voltage profile consisting of a normal polarity region and a reversed polarity region. Having this ability is important because normal polarity or reverse polarity alone may not be capable of analyzing a sample with a wide range of pIs, including those which are extremely acidic or basic, because it may not be possible to choose a pH in which all proteins are the same charge due loss of activity at extreme pHs²⁵. Instead, a pH closer to neutral pH can be used.

Lastly, the field for the dual polarity separation will be modified “on-the-fly” so that the two focused proteins will migrate through each other and ultimately switch positions within the separation channel. This is possible because of the ability to dynamically control the shape of the electric field in DFGF. Though it may be desired to switch the positions of species and elute them in opposite order, the important aspect of this demonstration is that the two species can be made to come into contact with each other. This opens up the possibility of new applications for performing on-column reactions, affinity assays, immunoassays, etc. An example of a possible application is briefly discussed in the Conclusions.

Experimental Section

Chemicals and Materials

R-phycoerythrin (R-PE), allo-phycoyanin (APC), Texas red conjugated ovalbumin (TR-OA) and a fluorescein isothiocyanate (FITC) protein labeling kit were purchased from Invitrogen (Carlsbad, CA). Cationized ferritin (CF), bovine serum albumin (BSA), cytochrome C (CYTC) and all other chemicals were obtained from Sigma-Aldrich (St. Louis, MO).

FITC-BSA was prepared according to the labeling kit instructions. After conjugation it was determined that each BSA contained approximately one FITC.

DFGF Apparatus

Experiments were conducted using a DFGF device (Figure 1A) that was previously described²⁰. Briefly, the chamber is formed from two 10.2 cm × 5.1 cm × 1.2 cm pieces of acrylic. A 5.7 cm × 0.1 cm × 500 μm channel is machined into one of the acrylic pieces and serves as the separation column. The other acrylic block has a 6.5 cm × 0.1 cm × 0.3 cm trough which contains the 21 platinum electrodes and a piece of porous ceramic (Kerafol, Germany). The ceramic is used to support a 6000 MWCO membrane (Spectrum Laboratories, Rancho Dominguez, CA) which isolates the separation channel from the electrodes by allowing the passage of current carrying ions while restricting the movement of target analytes. Purge buffer is pumped through the bottom block to remove joule heat and electrolysis products.

A syringe pump (KD Scientific, Holliston, MA, USA) fitted with a 250 μL glass Hamilton syringe (Hamilton, Reno, NV, USA) controls the flow of the running buffer through the separation column. Protein samples are injected into the separation channel using a two-position Cheminert VICI valve with microelectric actuation (Valco Instruments Co, Inc., Houston, TX, USA) equipped with a 10 μL sample loop. The flow rate was initially set at 0.8 μL/min to speed sample introduction. After 3 min, the flow was reduced to 0.15 μL/min and the sample was focused for 2 hrs. Electropherograms were collected by eluting focused

peaks through a UV-Vis detector (model: Linear 206 PHD). Moment analysis was then used to analyze the performance of the separation.

Based on linear mathematical modeling, the resolution, R_s , between two focused peaks can be determined from²⁶

$$R_s = \frac{|\Delta\mu_i|}{4\langle\mu_i\rangle} \frac{Q_i/(wh)}{\sqrt{\langle\mu_i\rangle D_i [dE_x/dx]}} \quad [1]$$

where $|\Delta\mu_i|$ is the difference in electrophoretic mobility, $\langle\mu_i\rangle$ is the average electrophoretic mobility, Q_i is the volumetric flow rate, w is the width of the separation channel, h is the height of the separation channel, D_i is the diffusion coefficient and dE_x/dx is the electric field gradient. From equation 1, one can see that, to increase the resolution, the electric field gradient, dE_x/dx , needs to be decreased, i.e. shallowed. Based on this linear theory, two species with a $|\Delta\mu_i|$ of $2 \times 10^{-6} \text{ cm}^2/(\text{V} \cdot \text{s})$ can be baseline separated ($R_s = 1$) in our DFGF device by shallowing the electric field gradient to 6 V/cm^2 . This corresponds to a difference in the electrophoretic mobilities of only 2.5%.

Voltage Controller

An improved DFGF controller was designed to be capable of applying both positive and negative electric fields within the focusing chamber while, at the same time, achieving a reduction in the footprint, weight, and power consumption compared to the previous voltage design²⁴. The new controller consists of 24 serially connected, independently controlled circuits. Each circuit has a ground level and a floating level, which are both isolated up to 4 kV. The ground level shares a common $\pm 15 \text{ VDC}$ power supply. For the floating level, each circuit has its own DC-DC floating power supply which is also $\pm 15 \text{ VDC}$. Each circuit uses an operational amplifier (op-amp) as its power output stage and has a full swing of approximately $\pm 14 \text{ VDC}$. The operational amplifier, a natural choice when a small foot print and high efficiency are required, can amplify an analog signal to handle higher power loads while maintaining excellent linearity. The maximum power output for each circuit is $\sim 0.5 \text{ W}$. Given an electrode pitch of 0.127 cm , the maximum field strength that could be achieved is 110 V/cm . Connected serially, the total voltage span across the 24 units could reach 350 V . The floating of the output stage makes it possible to establish a field gradient of arbitrary shape, i.e., any combination of positive and negative segments. The circuits are capable of electric field polarity switching on-the-fly. The control algorithm is based on the previous generation controller with the addition of dual polarity field gradient control. A graphical user interface (GUI) was developed using Labview 6.0 (National Instruments, Austin, TX). The user specifies the electric field profile, which is converted to voltage at each of the 24 units. The voltage profile is maintained by the program using a feedback control loop.

Results and Discussion

Normal Polarity Separations

Since a new voltage controller had been built which yields smaller electric fields, and thus shallower electric field gradients compared to the previously described controller²⁴, we tested the system by first performing a normal polarity separation. For this set of experiments, a sample of $0.3 \text{ } \mu\text{g}/\mu\text{L}$ of FITC-BSA ($\text{pI} \sim 4.8$), $0.1 \text{ } \mu\text{g}/\mu\text{L}$ of R-PE ($\text{pI} \sim 4.1$) and $0.1 \text{ } \mu\text{g}/\mu\text{L}$ of APC ($\text{pI} \sim 4.2$) was examined. A linear electric field gradient with a top-end electric field strength of 55.1 V/cm was initially set (Figure 1B). This produces a system consisting of 20 electrodes being anodes and the final being the cathode. The buffer was 20

mM Tris phosphate (pH 8.5) with 5 mM KCl. At this pH, the proteins all have a negative net charge.

After the sample was injected into the device and focused for 2 hrs, the peaks were eluted by first shallowing the electric field gradient to 27.56 V/cm over 60 min to increase resolution. The peaks were then mobilized past the detector according to the elution procedure outlined by Burke and Ivory²⁰. Briefly, the proteins were eluted by shifting the linear field towards the outlet while maintaining the same slope. This is accomplished by dropping the top-end electric field by 2.36 V/cm while at the same time adjusting the remaining electrodes to maintain the electric field gradient. Changes to the electric field were made every 5 min. Using this procedure ensured that the peaks maintained their concentration and resolution for the remainder of the elution protocol. A set of three repeats was run and electropherograms were collected. The detector was set to collect data at the wavelength of maximum absorbance of each of the proteins, which corresponded to 480 nm, 565 nm and 650 nm for FITC-BSA, R-PE and APC, respectively.

Prior to analysis, the electropherogram peaks were baseline-corrected by subtracting out drift, which was assumed to be linear, in the immediate neighborhood of the eluted peak²⁷. In addition, because the proteins' absorption spectra overlapped to a small degree at the monitored wavelengths, the overlapping spectra resulted in false peaks or tails. To adjust for this, the absorbance ratios at each monitored wavelength were calculated from a non-overlapping peak front or peak tail and these ratios were then fit to a line. Using this linear calibration curve, the overlapping contribution of each protein was subtracted from the main absorbance signal. It should be noted that this method will not work well if the peaks severely overlap; in that case a calibration curve would have to be generated in a separate experiment. Finally, moment analysis was performed on the baseline-corrected peaks to determine initial mass (m_0), elution time (t_m), peak standard deviation (σ) and resolution^{28, 29}.

The results of the normal polarity separation are shown in Figure 2. The three peaks are well formed and nearly Gaussian in shape with good resolution obtained for all three. Examination of the results of the moment analysis (Figure 2B) shows a resolution of 1.3 between the APC and R-PE and a resolution of 0.9 between the R-PE and the FITC-BSA. Though the resolution obtained in this case is adequate for our purpose, it may not be adequate for some applications. To increase the resolution further, the electric field would need to be shallowed before mobilizing the bands past the detector.

This example illustrates the ability to dynamically change the shape of the electric field profile in DFGF, one of the important advantages of DFGF over other EFGF devices. Under the initial focusing conditions, the resolution between the three proteins was not adequate and so the slope of the electric field was shallowed. If the peaks were eluted by continually shallowing the electric field (voltage controlled elution), as in the case of other EFGF devices, the result would yield overly resolved peaks with larger peak widths and decreased peak concentrations. With DFGF, however, the field can be initially shallowed to achieve the desired resolution and then the bands can be mobilized past the detector while maintaining the slope of the electric field. This ensures that the peaks retain their shape, concentration and resolution during the remainder of the elution protocol.

The reproducibility between the three experimental runs was very good showing little run-to-run variation, and the elution times of the three proteins varied less than 1% between the runs. There was slightly more variation in σ between the runs, with the FITC-BSA exhibiting the greatest change in σ at 9%, and the R-PE and APC varying by only 3.5% and 6.2%, respectively.

Reversed Polarity Separations

In some cases, operating at alkaline pH is not possible due either to the high pIs of some analytes which would require an extremely high operating pH or due to the pH stability of the target species. When attempting these separations, operating at acidic or neutral pH would be beneficial. In addition, operating at sufficiently low pH has other advantages in that, at lower pH, the surface charges on the wall and in the chromatographic packing will decrease or turn off and the amount of electroosmotic flow (EOF) within the system will decline²⁵. This is particularly important in EFGF because the gradient in the electric field produces an EOF profile that varies along the length of the separation channel³⁰. This becomes problematic when eluting focused bands through the outlet of the separation channel because the peak concentration, peak shape and resolution will change with the flow profile due to variations in EOF along the length of the channel.

When operating under acidic conditions, most proteins are positively charged. In order to separate and concentrate these species, reversed polarity fields (negative voltages) are needed. To illustrate the capability of the new voltage controller to perform reversed polarity separations, a series of three experiments were run. A linear electric field was used with an electric field strength of -53.5 V/cm at the inlet (Figure 1B). In this case the electrode array consisted of 20 cathodes and 1 anode. A protein sample of 0.2 mg/mL CF (pI ~ 8.5) and 0.2 mg/mL TR-OA (pI ~ 4.6) in 5 mM Tris phosphate (pH 3.08) buffer with 5 mM KCl was injected into the separation channel at 0.8 μ L for 3 min. The flow was then reduced to 0.15 μ L/min and the proteins were focused for 2 hrs. In this case, sufficient resolution was obtained using this field profile and so focused peaks were eluted while maintaining the slope of the electric field according to the procedure described above. The CF and TR-OA were monitored at 380 nm and 590 nm, respectively, and collected electropherograms were analyzed in the same fashion as the normal polarity separations described above.

The electropherogram in Figure 3A illustrates the successful separation of TR-OA and CF under acidic conditions. The reproducibility for this system was very good. The moment analysis (Figure 3B) shows that a resolution of 0.9 ± 0.05 was obtained corresponding to a variation of only 5% between the different runs. As with the normal polarity separation, the calculated elution times were very reproducible with the difference being less than 1% for both of the proteins.

Dual Polarity Separations

To perform dual polarity experiments, the voltage applied to the separation channel was split into normal polarity and reversed polarity regions, allowing for the simultaneous separation of negatively and positively charged species. Figure 1C shows the voltage profile and the corresponding electric field profile applied to this system. A sample of 0.1 μ g/ μ L R-PE and 0.5 μ g/ μ L CYTC was injected at 0.8 μ L/min for 3 min. The flow was then reduced to 0.1 μ L/min. The buffer used in this case was 10 mM Tris phosphate (pH 7.2) with 15 mM KCl. At this pH, the R-PE is negatively charged (pI ~ 4.1) and the CYTC is positively charged (pI ~ 10). After 2 hrs, the samples were eluted past the detector using an elution protocol that maintained the electric field gradient in both the normal polarity and reversed polarity regions of the separation channel. A set of three experiments were run and electropherograms collected. The detector was set to monitor 400 nm and 565 nm for the CYTC and R-PE, respectively.

A representative electropherogram is shown in Figure 4A. There is very good separation between the CYTC and the R-PE which is to be expected since the two proteins were isolated into different regions of the separation channel. Unexpectedly, two CYTC peaks, a major and a minor peak, were present. These most likely represent the reduced and oxidized

forms of CYTC³¹. To ensure that the two peaks were in fact CYTC and not due to an artifact of the system, gradient elution cation exchange chromatography on Sepharose SP FF was run. The results (data not shown) confirmed the presence of the two CYTC peaks.

To determine the reproducibility of the separation, moment analysis was performed on the electropherograms. As with the previous experiments, baseline drift and contributions of the peaks to other wavelengths was adjusted. However, in this case, the presence of the major and minor peaks of CYTC complicates the analysis because the two peaks overlap. In previous experiments, overlapping peaks were not an issue because each peak was monitored at a separate wavelength. When the peaks overlapped, as is the case in Figure 2A and Figure 3A, they were easily deconvoluted by subtracting out the contributions of each peak to the other wavelength. However, with the CYTC, the major and minor peaks were monitored at the same wavelength and so a more traditional and complicated deconvolution algorithm would need to be used. In general, deconvolution algorithms are difficult to employ²⁷ and their application lies outside the scope of this paper.

In our case, moment analysis is used mainly to illustrate the reproducibility of the system and so a rougher, less quantitative approach was used. Moment analysis was performed by integrating the major peak from its leading edge to the valley between the two peaks. The analysis on the minor peak was performed by integrating from the valley to its trailing edge. Though the values obtained using this technique are inaccurate, they are sufficient to show reproducibility. Lastly, the resolution between the peaks was determined using a triangulation technique²⁹.

The results of the moment analysis are shown in Figure 4B. As with the previous experiments, the reproducibility of the dual polarity system is very good. The t_m and σ for each of the peaks are less than 1% and 4% variation, respectively. The mass balance, m_0 , for the CYTC shows the largest variation between the different runs. This is likely due to a small amount of sticking onto the surface of the chromatographic packing. However, the results still agree within 15%.

In practice, the simultaneous separation and concentration of negatively and positively charged species does not need to be performed within the same apparatus. Instead, a tandem setup similar to the one illustrated by Lin et al.³² can be used except that one device would be operated under normal polarity conditions and the other operated under reversed polarity conditions. In this manner, the positively and negatively charged species would be focused in different apparatuses.

However, in a DFGF system, having the species focused simultaneously within the same device provides the operator with the unique ability to manipulate the field in such a way that the positions of the focused peaks can be manipulated “on-the-fly”, e.g. switched. Though it may be desired to elute the species in opposite order, the real advantage of this capability is that the analytes can be made to contact each other. This would allow for performing on-column reactions, protein-protein interactions, immunoassays or affinity assays.

Figure 5A shows the CYTC and R-PE bands under the initial focusing conditions, with the CYTC near the outlet and R-PE near the inlet. Under a traditional elution protocol, the CYTC would be eluted first followed by the R-PE and an electropherogram similar to Figure 4A would be obtained. However, if instead, the electric field profile is changed to move the CYTC towards the inlet (Figure 5B), the two protein bands can be passed through each other (Figure 5C) such that they eventually switch positions (Figure 5D). The electric field can then be switched to capture the R-PE at the outlet and to maintain the CYTC at the inlet (Figure 5E). The field in this case is a mirror image along the x-axis of the profile

shown in Figure 1C. The proteins can then be eluted past the detector in the reverse order to the previous illustration.

The electropherogram is shown in Figure 5F. One interesting thing to note is that only one CYTC band is observed. It is likely that the resolution between the major and minor band is lost during elution due to band spreading caused by adsorption onto the chromatographic packing. For the results obtained in Figure 4A, the CYTC was focused near the outlet such that during elution it only migrated a short distance before passing by the detector. This limited the impact that adsorption had on the focused peak. However, when the positions of the bands were switched, the CYTC had to migrate through the entire channel and the effect of adsorption became more evident. We have already seen evidence of CYTC sticking to the packing as indicated by the larger variations in m_0 seen in Figure 4B. One possible solution to this problem would be to add a nonionic surfactant to the running buffer to reduce adsorption.

Though the protocol for migrating the focused peaks though each other needs to be further optimized to minimize some of these problems and to determine optimal run conditions, we have shown that using a DFGF apparatus with a voltage controller capable of operating under normal and reversed polarity affords the researcher more flexibility with respect to the types of analyses that can be performed.

Conclusions

This paper introduced a new voltage controller which is capable of normal polarity or reversed polarity for the separation of negatively or positively charged species in DFGF. First, experiments were conducted while operating at alkaline pH (pH 8.5) under normal polarity conditions. In this case, positive potentials were applied to the electrodes, which behaved as anodes, with the electrode closest to the outlet being the cathode. The successful separation of FITC-BSA, R-PE and APC was illustrated and moment analysis performed on the electropherograms showed less than 1% run-to-run variation in t_m for each of the proteins and only 9%, 3.5% and 6.2% change in σ for the FITC-BSA, R-PE and APC, respectively.

Experiments were then conducted in pH 3.08 buffer. At this pH, the proteins, CF and TR-OA, were positively charged so that the system needed to be operated under reversed polarity with negative potentials applied to the electrodes with 20 of those being cathodes and one an anode. As with the normal polarity separation, the results obtained under reversed polarity showed very good reproducibility with less than 1% run-to-run variation in the t_m .

Next, the DFGF system was operated near neutral pH (pH 7.2). At this pH, the protein sample consisted of a negatively charged species (R-PE) and a positively charged species (CYTC). This separation was not previously possible in DFGF; however, the new voltage controller was designed is capable of any combination of positive and negative segments. As a result, an electric field consisting of normal polarity and reversed polarity regions could be established. The results from this separation showed that negatively and positively charged species could be simultaneously separated within the same device and then individually eluted.

Lastly, the electric field was changed in such a way as to migrate the two oppositely charged proteins, R-PE and CYTC, such that they came into contact with each other, switched positions within the separation channel and eluted in opposite order. This is possible because the electric field profile in DFGF can be dynamically varied during the course of an experiment. Such a manipulation of the field and focused protein bands is not possible in

any other EFGF technique. The fact that the proteins can be made to pass through each other opens up the possibility of other analyses that could be performed in DFGF, including on-column reactions, investigation into protein-protein or antigen-antibody interactions, or affinity assays.

As a possible example, a complex mixture of proteins could be held in a DFGF operating under normal polarity such that all the species being focused are negatively charged. The field could then be changed to dual polarity and a phosphorylation state-specific antibody^{33, 34} designed to carry a large positive charge is injected into the column. As the antibody binds to the phosphorylated proteins, the complex takes on a positive charge and migrates into the reversed polarity section of the channel. Any proteins not containing phosphorylation can be removed from the sample by switching the entire separation channel to reversed polarity. Since the unbound proteins would still be negatively charged they will not focus and will be flushed out of the device, leaving only the positively charged antibody-protein complexes. The phosphorylated proteins can then be fractionated further or individually eluted for off-column analysis.

Though this type of analysis has not yet been performed experimentally, the development of the controller introduced in this paper opens up these possibilities. We anticipate the publication of these alternative applications of DFGF in the near future.

Acknowledgments

The authors gratefully acknowledge Washington State University National Institutes of Health Protein Biotechnology Training Program (grant TM2GM08336) and Pfizer Inc. for funding.

References

1. Huang Z, Ivory CF. *Analytical Chemistry*. 1999; 71:1628–1632.
2. Koegler WS, Ivory CF. *Biotechnology Progress*. 1996; 12:822–836.
3. Humble PH, Kelly RT, Woolley AT, Tolley HD, Lee ML. *Analytical Chemistry*. 2004; 76:5641–5648. [PubMed: 15456281]
4. Koegler WS, Ivory CF. *Journal of Chromatography A*. 1996; 726:229–236.
5. Liu J, Sun X, Fransworth PB, Lee ML. *Anal Chem*. 2006; 78:4654–4662. [PubMed: 16808478]
6. Greenlee RD, Ivory CF. *Biotechnology Progress*. 1998; 14:300–309. [PubMed: 9548784]
7. Wang QG, Lin SL, Warnick KF, Tolley HD, Lee ML. *Journal of Chromatography A*. 2003; 985:455–462. [PubMed: 12580514]
8. Hoebel SJ, Balss KM, Jones BJ, Malliaris CD, Munson MS, Vreeland WN, Ross D. *Analytical Chemistry*. 2006; 78:7186–7190. [PubMed: 17037919]
9. Kim SM, Sommer GJ, Burns MA, Hasselbrink EF. *Analytical Chemistry*. 2006; 78:8028–8035. [PubMed: 17134136]
10. Matsui T, Franzke J, Manz A, Janasek D. *Electrophoresis*. 2007; 28:4606–4611. [PubMed: 18008305]
11. Munson MS, Danger G, Shackman JG, Ross D. *Analytical Chemistry*. 2007; 79:6201–6207. [PubMed: 17616169]
12. Ross D, Locascio LE. *Analytical Chemistry*. 2002; 74:2556–2564. [PubMed: 12069237]
13. Shackman JG, Munson MS, Ross D. *Analytical and Bioanalytical Chemistry*. 2007; 387:155–158. [PubMed: 17102967]
14. Myers P, Bartle KD. *Journal of Chromatography A*. 2004; 1044:253–258. [PubMed: 15354445]
15. Petsev DN, Lopez GP, Ivory CF, Sibbett SS. *Lab on a Chip*. 2005; 5:587–597. [PubMed: 15915250]
16. Tracy NI, Huang Z, Ivory CF. *Biotechnology Progress*. 2008; 24:444–451. [PubMed: 18225913]
17. Tracy NI, Ivory CF. *Journal of Separation Science*. 2008; 31:341–352. [PubMed: 18196522]

18. Tracy NI, Ivory CF. *Electrophoresis*. 2008; 29:2820–2827. [PubMed: 18615787]
19. Tracy NI, Ivory CF. *Aiche Journal*. 2009; 55:63–74.
20. Burke JM, Ivory CF. *Electrophoresis*. 2008; 29:1013–1025. [PubMed: 18306183]
21. Burke JM, Ivory CF. Accepted to *Electrophoresis*. 2009
22. Tunon PG, Wang Y, Myers P, Bartle KD, Bowhill L, Ivory CF, Ansell RJ. *Electrophoresis*. 2008; 29:457–465. [PubMed: 18064598]
23. Lin SL, Li Y, Woolley AT, Lee ML, Tolley HD, Warnick KF. *Electrophoresis*. 2008; 29:1058–1066. [PubMed: 18246576]
24. Huang, Z. PhD Thesis. Washington State University; Pullman, WA: 2001.
25. Righetti, PG. *Capillary electrophoresis in analytical biotechnology*. CRC Press; Boca Raton: 1996.
26. Ivory, CF. *Handbook of Isoelectric Focusing and Proteomics*. Garfin, D.; Ahuja, S., editors. Vol. 7. Elsevier Inc; San Diego: 2005.
27. Nikitas P, Pappa-Louisi A, Papageorgiou A. *Journal of Chromatography A*. 2001; 912:13–29. [PubMed: 11307976]
28. Brown, PR.; Hartwick, RA., editors. *High Performance Liquid Chromatography*. John Wiley & Sons, Ltd; 1989.
29. Dyson, NA. *Chromatographic integration methods*. 2. Royal Society of Chemistry, Information Services; Cambridge: 1998.
30. Maynes D, Tenny J, Webb BW, Lee ML. *Electrophoresis*. 2008; 29:549–560. [PubMed: 18200632]
31. He T, Chandramouli N, Fu E, Wu A, Wang YK. *Anal Biochem*. 1999; 271:189–192. [PubMed: 10419636]
32. Lin SL, Li YY, Tolley HD, Humble PH, Lee ML. *Journal of Chromatography A*. 2006; 1125:254–262. [PubMed: 16828105]
33. Goto H, Inagaki M. *Nature Protocols*. 2007; 2:2574–2581.
34. Mandell JW. *American Journal of Pathology*. 2003; 163:1687–1698. [PubMed: 14578166]

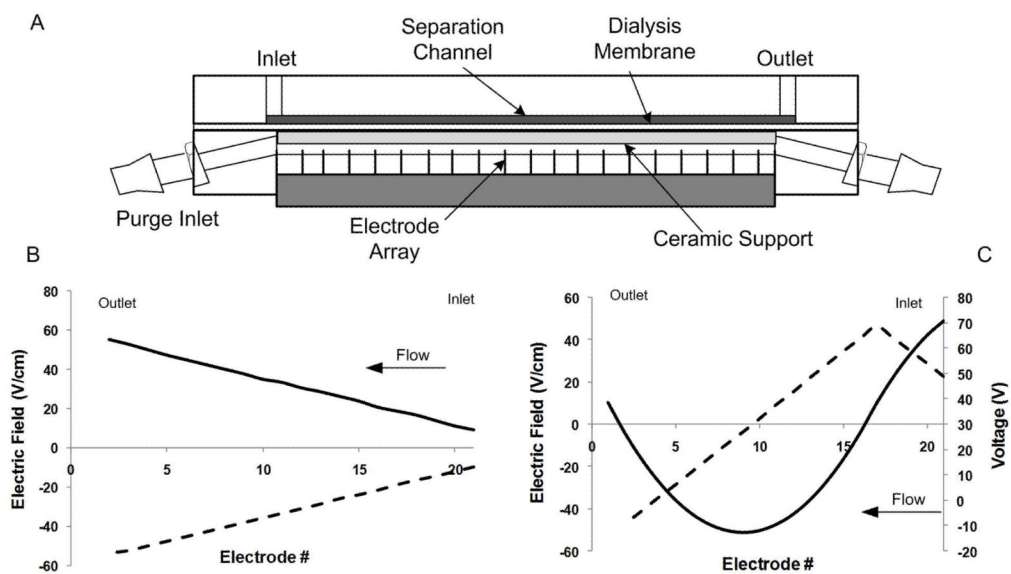


Figure 1. (A) DFGF device schematic. (B) Electric field profile for the normal polarity separations (solid line) and reversed polarity separations (dashed line). (C) Voltage profile (solid line) and corresponding electric field profile (dashed line) for the dual polarity separation of negatively and positively charged proteins.

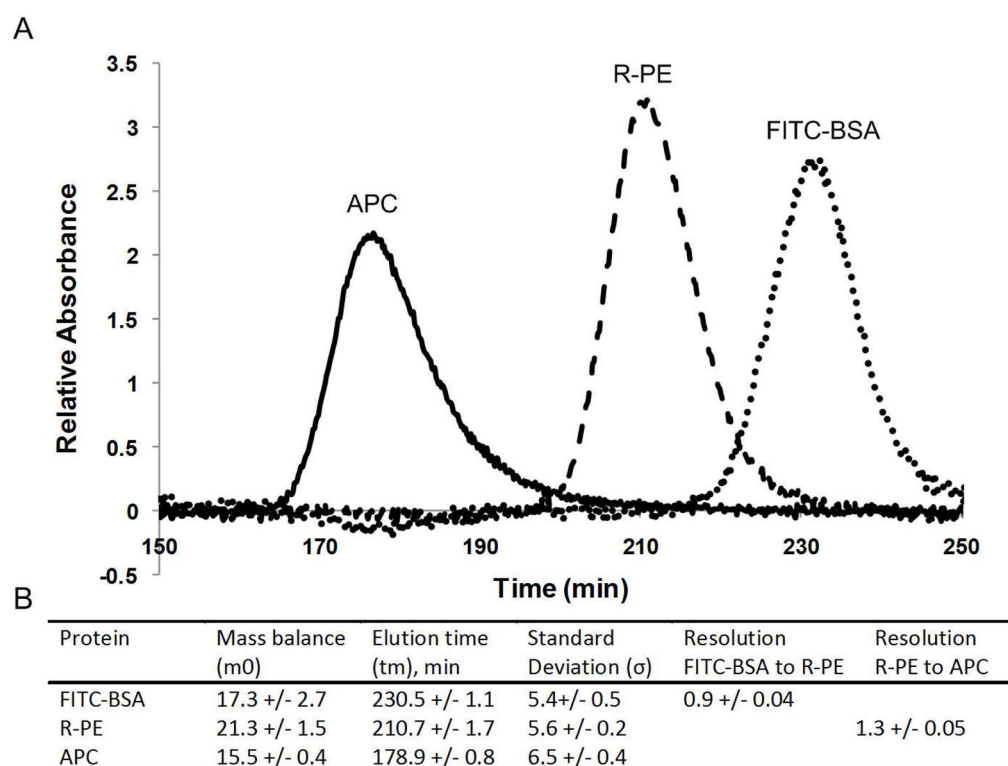


Figure 2. Normal polarity experimental results. (A) Representative electropherogram showing the separation of FITC-BSA, R-PE and APC. (B) Moment analysis results. The three experimental runs show very good reproducibility with the retention times of each the peaks showing less than 1% run-to-run variation. The peak standard deviations (σ) exhibit more run-to-run variation, but still agree within 10%.

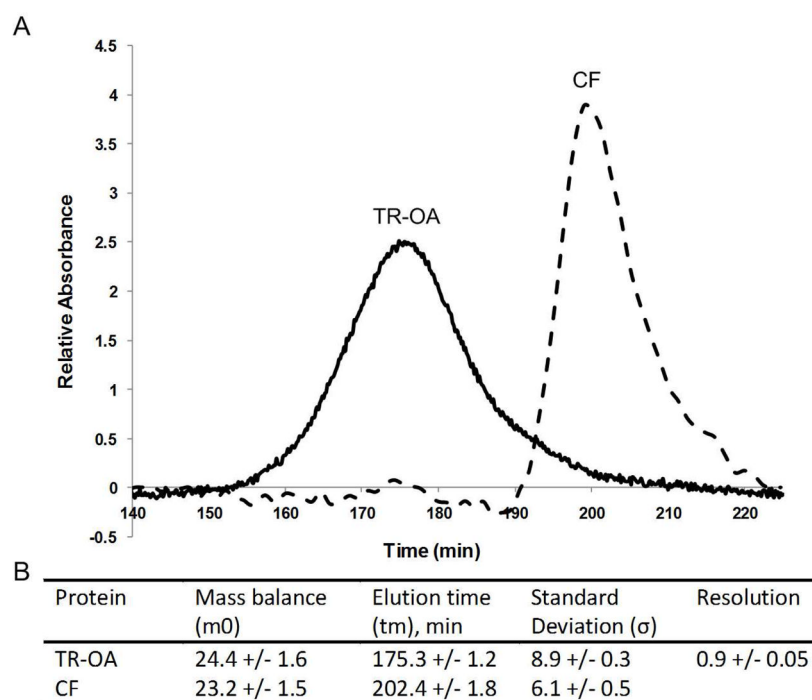


Figure 3. (A) Representative electropherogram of the reversed polarity separation of texas red conjugated ovalbumin (TR-OA) and cationized ferritin (CF). (B) Moment analysis results. The reproducibility of this system is very good with the elution times of each protein showing less than 1% variability between the three different runs. The resolution between the two peaks was calculated to be 0.9.

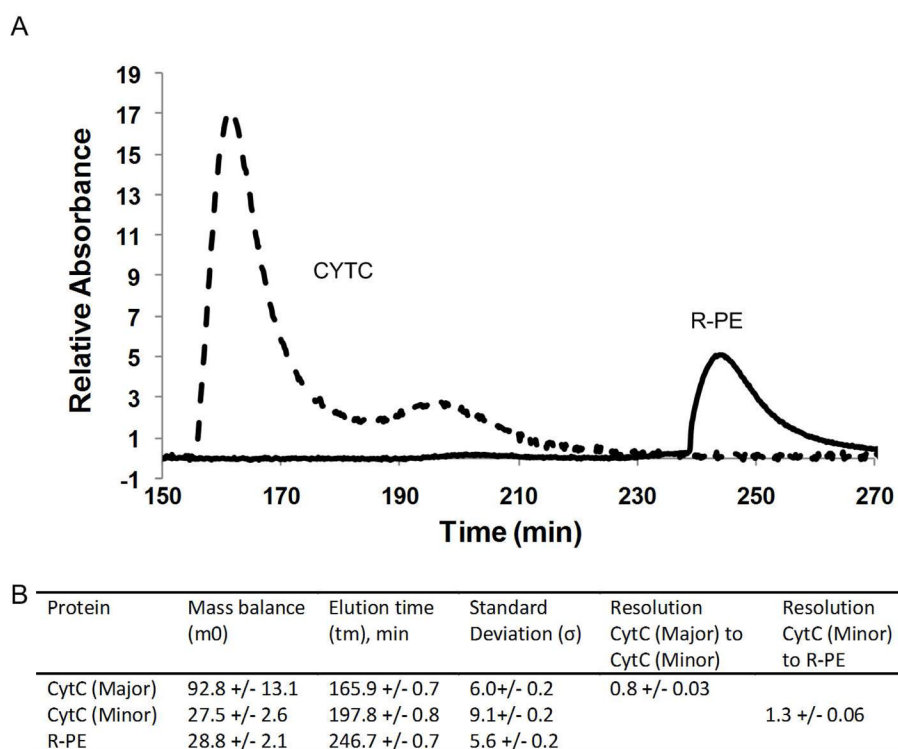


Figure 4. Representative electropherogram for the dual polarity separation of positively charged cytochrome c (CYTC) and negatively charged (R-PE). This results shows that the new controller can be used for the simultaneous separation of negatively and positively charged species. In addition, the CYTC was resolved into a major and minor peak, likely the oxidized and reduced form. (B) Moment analysis results for the dual polarity separation.

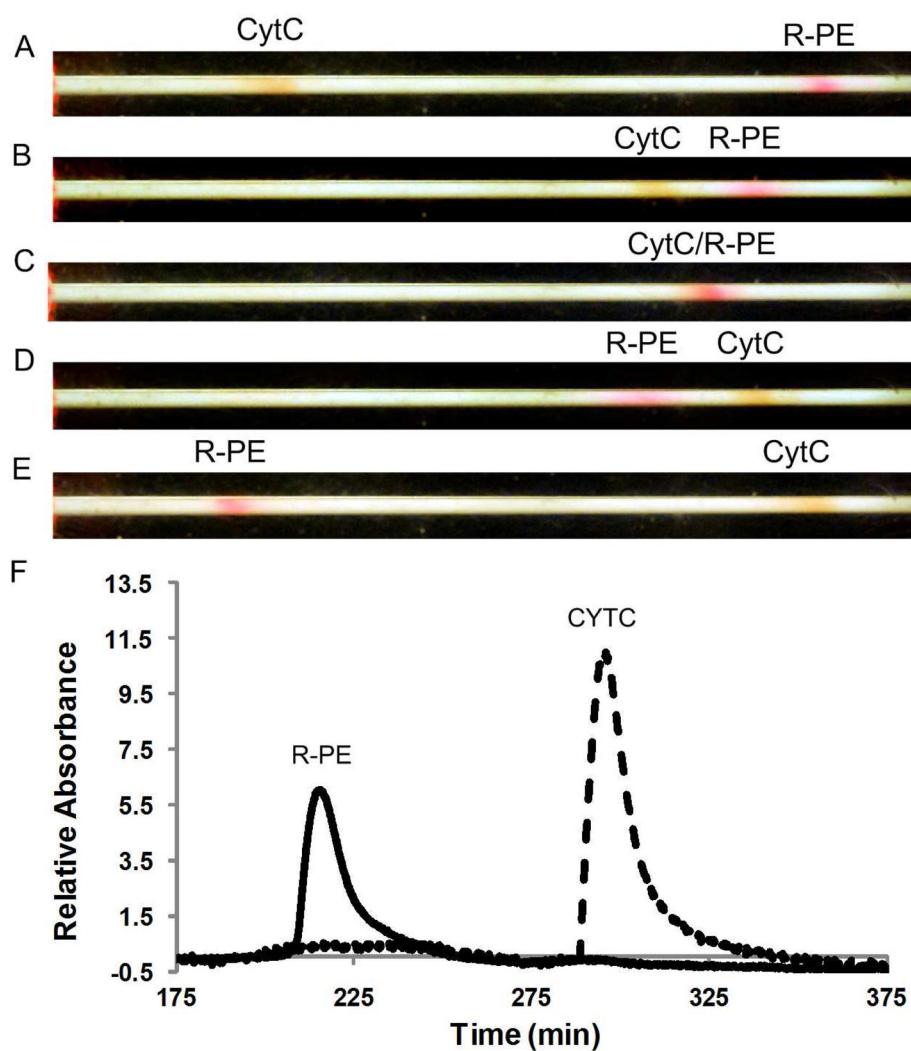


Figure 5. Dual polarity separation of CYTC (positively charged) and R-PE (negatively charged). (A) Initial focusing conditions represented by electric field profile in Figure 3A. (B) Field is changed to move CYTC towards the inlet. (C) CYTC and R-PE passing through each other. (D) Peaks have switched positions and the field is changed to maintain the CYTC at the inlet and to capture the R-PE at the outlet. (E) Final focusing conditions prior to eluting both peaks past the detector. (F) Electropherogram for the dual polarity separation with the CYTC and R-PE switched.